Inorg. Chem. **2008**, *47*, 6014−6027

Simple, Nitrogen-Rich, Energetic Salts of 5-Nitrotetrazole

Thomas M. Klapötke,* Peter Mayer, Carles Miró Sabaté, Jan M. Welch, and Nikolai Wiegand

Department Chemistry and Biochemistry, Ludwig-Maximilians-Universität München, Butenandtstrasse 5-13, D-81377 München, Germany

Received February 25, 2008

A new family (ammonium, **1**, hydrazinium, **2**, guanidinium, **3**, aminoguanidinium, **4**, diamino-guanidinium, **5**, and triaminoguanidinium, **6**) of simple, nitrogen-rich energetic salts based on 5-nitro-2*H*-tetrazole (HNT) were synthesized. In addition, the hemihydrate of **1** (**1a**) and the hydrate of **6** (**6a**) were also isolated. In all cases, stable salts were obtained and fully characterized by vibrational (IR, Raman) spectroscopy, multinuclear (^{1}H, ^{13}C and ^{14}N) NMR spectroscopy, mass spectrometry, elemental analysis, and X-ray structure determination. Compounds **1**and **2** crystallize in the monoclinic space group $P2_1/c$, **1a** and **3** crystallize in $C/2c$, **4** in $P2_1/n$, **5** in $P2_1$, **6** in orthorhombic $P2_12_12_1$, and **6a** in triclinic $P\bar{1}$. Initial safety testing (impact, friction, and electrostatic sensitivity) and thermal stability measurements (DSC) were also carried out. The NT salts all exhibit good thermal stabilities (decomposition above 150 °C). The constant volume energies of combustion (Δ_cU(exp)) of **1**−**6** were experimentally determined by oxygen bomb calorimetry to be −1860(30) cal/g (**1**), −1770(30) cal/g (**1a**), −2110(150) cal/g (**2**), −2250(40) cal/g (**3**), −2470(30) cal/g (**4**), −2630(40) cal/g (**5**), −2690(50) cal/g (**6**), and −2520(50) cal/g (**6a**). Because of the significant experimental uncertainties obtained in these measurements, their validity was checked by way of quantum chemical calculation (MP2) of electronic energies and an approximation of lattice enthalpy. The predicted constant volume energies of combustion (Δ_cU(pred)) calculated by this method were −2095.9 cal/g (**1**), −1975.7 cal/g (**1a**), −2362.4 cal/g (**2**), −2526.6 cal/g (**3**), −2654.6 cal/g (**4**), −2778.6 cal/g (**5**), −2924.0 cal/g (**6**), and −2741.4 cal/g (**6a**). From the experimentally determined density, chemical composition, and energies of formation (back calculated from the heats of combustion) the detonation pressures and velocities of **1** (7950 m/s, 23.9 GPa), **1a** (7740 m/s, 22.5 GPa), **2**(8750 m/s, 30.1 GPa), **3** (7500 m/s, 20.1 GPa) **4**(8190 m/s, 24.7 GPa), **5**(8230 m/s, 24.4 GPa), **6** (8480 m/s, 26.0 GPa) and **6a** (7680 m/s, 20.7 GPa) were predicted using the EXPLO5 code.

Introduction

In the development of energetic materials, increased performance with decreased sensitivity to physical stimuli is sought. Unfortunately, performance and sensitivity are linked both to each other and to general physical and chemical properties, most significantly enthalpy of formation (Δ_fH), density (ρ), and oxygen balance (Ω). One way of counteracting the correlation of high performance (detonation pressure and detonation velocity) with high sensitivity to impact, friction, and shock is the use of systems such as 1,1-amino-2,2-dinitroethene (FOX-7)[1–4] or 1,3,5-triamino-2,4,6-trinitrobenzene,[5] which form extensive hydrogen bonding networks in the solid state. Such hydrogen bond networks (especially between amino and nitro groups) help to stabilize the material substantially. In addition to lower sensitivities, the performance of such materials is generally adequate because the chemical composition (FOX-7, for example, shares a common empirical formula, $CH_2N_2O_2$, with HMX and RDX) is unaffected by strong hydrogen bonding, density is generally increased, and heat of formation slightly decreased (less positive). Because the performance of an energetic material is most heavily dependent on density, increases in density tend to outweigh the adverse affect on heat of formation caused by strong hydrogen bonding.

* To whom correspondence should be addressed. E-mail: tmk@cup.uni-muenchen.de. Fax: +49 89 2180 77492.

(1) Latypov, N. V.; Bergman, J.; Langlet, A.; Wellmar, U.; Bemm, U. *Tetrahedron* **1998**, *54*, 11525–11536.
(2) Bemm, U.; Östmark, H. *Acta Crystallogr.* **1998**, *C54*, 1997–1999.
(3) Evers, J.; Klapötke, T. M.; Mayer, P.; Oehlinger, G.; Welch, J. *Inorg. Chem.* **2006**, *45*, 4996–5007.
(4) Bellamy, A. J. FOX-7 (1,1-Diamino-2,2-dinitroethene). In *High Energy Density Materials*, 1st ed.; Klapötke, T. M., Ed.; Springer-Verlag: Berlin, 2007; *125*, 1−33; Structure & Bonding.
(5) Cady, H. H.; Larson, A. C. *Acta Crystallogr.* **1965**, *18*, 485–496.

10.1021/ic800353y CCC: $40.75 © 2008 American Chemical Society
Published on Web 06/07/2008

Ionic energetic materials based on amines, hydrazines, and guanidines are also known to form strong hydrogen bonding networks and can show remarkable stability and considerable insensitivity to physical stimuli, as well as good explosive performance. In addition, known ammonium, hydrazinium, and guanidinium salts are composed mainly of nitrogen and thus have large positive enthalpies of formation, as well as densities comparable to or greater than those of widely used neutral, covalent, organic explosives. Salts such as ammonium nitrate, perchlorate, and dinitramide are commonly used as oxidizers in explosive and propellant mixtures. In addition, the oxygen balances of guanidine salts are only slightly negative when an oxygen-rich counteranion (perchlorate, nitrate, and dinitramide) is used. Furthermore, ionic energetic materials tend to exhibit lower vapor pressure (essentially eliminating the risk of exposure through inhalation) than similar neutral nonionic analogues.[6–8] With these properties in mind, simple, nitrogen-rich (ammonium, hydrazinium and guanidinium based) salts of 5-nitro-2*H*-tetrazole have been investigated as potential new, low-sensitivity energetic materials.

The 5-nitrotetrazolate anion (NT^-) was first synthesized over 75 years ago by von Herz. Since its discovery, the metal and heavy metal salts of HNT have attracted much interest as primary explosives.[9–13] More recently metal complexes (Zn and Fe) have been suggested as potential "green" replacements for lead azide in initiators.[14] In 1998 the free acid of the NT^- anion was isolated and characterized for the first time along with a series of functionalized derivatives.[15] Additional, neutral energetic derivatives have also appeared over the past few years.[16] Finally, also in recent years, new energetic heterocycle based salts of HNT have appeared in the literature, many of which display ionic liquid properties.[6,8,17–20] Considering the amount of literature on the subject and the recent interest in the area of ionic energetic materials (both liquid and solid), we were surprised to find that the simplest metal-free nitrogen-rich salts of HNT remained largely uninvestigated. Here we present the syntheses from simple, inexpensive materials, full characterization, and initial safety testing and predicted energetic performance of a series of these previously under-investigated materials.

Experimental Section

Caution! *5-nitro-2H-tetrazole, and its derivatives are energetic materials and tend to explode under certain conditions. Appropriate safety precautions should be taken, especially when these compounds are prepared on a larger scale or placed under physical stress (i.e., pressing KBr or benzoic acid pellets). Laboratories and personnel should be properly grounded, and safety equipment such as Kevlar gloves, leather coats, face shields, ear plugs, as well as blast screens, are highly recommended.*

General Description. All chemical reagents and solvents were obtained from Sigma-Aldrich Inc. or Acros Organics (analytical grade) and were used as supplied. 1-Amino-2-ammonioguanidinium sulfate and 1,2,3-traminoguanidinium hemisulfate dihydrate were prepared by treatment of 1,3-diaminoguanidinium chloride with 1 equiv of sulfuric acid in water and ion exchange chromatography, respectively. ^{1}H, ^{13}C, and ^{14}N NMR spectra were recorded on a JEOL Eclipse 400 instrument in DMSO-d_6 at or near 25 °C. The chemical shifts are given relative to tetramethylsilane (^{1}H, ^{13}C) or nitromethane (^{14}N) as external standards, and coupling constants are given in hertz (Hz). Infrared (IR) spectra were recorded on a Perkin-Elmer Spectrum One FT-IR instrument as KBr pellets at 20 °C. Transmittance values are qualitatively described as "very strong" (vs), "strong" (s), "medium" (m), and "weak" (w). Raman spectra were recorded on a Perkin-Elmer Spectrum 2000R NIR FT-Raman instrument equipped with a Nd:YAG laser (1064 nm). The intensities are reported as percentages of the most intense peak and are given in parentheses. Elemental analyses were performed with a Netsch Simultaneous Thermal Analyzer STA 429. Melting points were determined by differential scanning calorimetry (Perkin-Elmer Pyris 6 DSC instrument, calibrated with standard pure indium and zinc). Measurements were performed at a heating rate of 10 °C/min in closed aluminum sample pans with a 1 μm hole in the top for gas release under a nitrogen flow of 20 mL/min with an empty identical aluminum sample pan as a reference.

Bomb Calorimetry. For all calorimetric measurements, a Parr 1356 bomb calorimeter (static jacket) equipped with a Parr 207A oxygen bomb for the combustion of highly energetic materials was used.[21] A Parr 1755 printer, furnished with the Parr 1356 calorimeter, was used to produce a permanent record of all activities within the calorimeter. The samples (~200 mg each) were carefully mixed with ~800 mg analytical grade benzoic acid and carefully pressed into pellets, which were subsequently burned in a 3.05 MPa atmosphere of pure oxygen. The experimentally determined heats of combustion were obtained as the averages of five single measurements with standard deviations calculated as a measure of experimental uncertainty. The calorimeter was calibrated by the combustion of certified benzoic acid in an oxygen atmosphere at a pressure of 3.05 MPa.

Synthesis of Ammonium 5-Nitrotetrazolate Hemihydrate (1a).[22] To a vigorously stirred mixture of 30 g of ice and 30 g of water in a 250 mL plastic beaker were added 5.5 g (22 mmol) copper (II) sulfate pentahydrate and 10.4 g (150 mmol) of sodium nitrite. The temperature was maintained at ~2 °C (ice water bath) and a previously prepared and cooled (~2 °C) solution of 4.25 g (50 mmol) of 5-aminotetrazole, 2.8 mL (50 mmol) of concentrated

(6) Xue, H.; Shreeve, J. M. *Adv. Mater. (Weinheim, Ger.)* **2005**, *17*, 2142–2146.
(7) Sikder, A. K.; Sikder, N. *J. Hazard. Mater.* **2004**, *112*, 1–15.
(8) Xue, H.; Twamley, B.; Shreeve, J. M. *Inorg. Chem.* **2005**, *44*, 7009–7013.
(9) Redman, L. D.; Spear, R. J. Report MRL-R-901; Materials Research Laboratory: Australia, 1983; pp 1−27.
(10) von Herz, E. U.S. Patent 2066954, 1937.
(11) Gilligan, W. H.; Kamlet, M. J. Report NSWC/WOL/TR 76−146; White Oak Laboratory: Silver Spring, MD, 1976; pp 1−15.
(12) Gilligan, W. H. U.S. Patent 4093623, 1977.
(13) Spear, R. J.; Elischer, P. P. *Aust. J. Chem.* **1982**, *35*, 1–13.
(14) Huynh, M. H. V.; Hiskey, M. A.; Meyer, T. J.; Wetzler, M. *Proc. Natl. Acad. Sci. U.S.A.* **2006**, *103*, 5409–5412.
(15) Koldobskii, G. I.; Soldatenko, D. S.; Gerasimova, E. S.; Khokhryakova, N. R.; Shcherbinin, M. B.; Lebedev, V. P.; Ostrovskii, V. A. *Russ. J. Org. Chem. (Engl. Trans.)* **1997**, *33*, 1771–1783.
(16) Boese, R.; Klapötke, T. M.; Mayer, P.; Verma, V. *Propellants, Explos., Pyrotech.* **2006**, *31*, 263–268.
(17) Gao, H.; Ye, C.; Piekarski, C. M.; Shreeve, J. M. *J. Phys. Chem.* **2007**, *C111*, 10718–10731.
(18) Xue, H.; Gao, H.; Twamley, B.; Shreeve, J. M. *Chem. Mater.* **2007**, *19*, 1731–1739.
(19) Xue, H.; Gao, H.; Twamley, B.; Shreeve, J. M. *Eur. J. Inorg. Chem.* **2006**, *15*, 2959–2965.
(20) Xue, H.; Gao, Y.; Twamley, B.; Shreeve, J. M. *Inorg. Chem.* **2005**, *44*, 5068–5072.
(21) http://www.parrinst.com.
(22) Lee, K. Y.; Coburn, M. D. *J. Energ. Mater.* **1983**, *1*, 109–122.

sulfuric acid, and a 0.2 g (0.8 mmol) of copper (II) sulfate in 70 mL of water (pale-blue solution). Addition resulted in vigorous gas evolution, as well as the formation of a frothy, pale blue-green solid. After addition was completed (~30 min), the dropping funnel was rinsed with ~20 mL of water and removed. The resulting blue-green slurry was allowed to stir at room temperature for 1 h. A 4.1 g (100 mmol) quantity of solid sodium hydroxide was then added to the vigorously stirred blue-green slurry resulting in a darkening of the solution (dark-blue slurry). The dark-blue slurry was then heated to ~70 °C for ~1 h with vigorous stirring to convert the blue copper (II) hydroxide to black-brown copper (II) oxide. The resulting brownish-green suspension was then filtered hot through an approximately 2 cm thick plug of celite wet-packed in a 110 mm plastic Büchner funnel. The celite was subsequently washed twice with 50 mL of hot water. The filtrate (clear greenish-yellow solution) was then acidified with 1.6 mL (~27 mmol) of concentrated sulfuric acid and treated with decolorizing carbon while warm. The addition of carbon resulted in gas evolution, and the resulting suspension was then stirred for ~15 min. The solution was once again filtered through a ~2 cm wet-packed plug of celite yielding a nearly clear (slightly yellow) solution. This solution was acidified with a further 1.6 mL (~27 mmol) of concentrated sulfuric acid, and then extracted with a solution of 12 mL (18.9 mmol) of tridodecylamine in 150 mL of dichloroethane in a separatory funnel. The aqueous layer was set aside and the organic phase (clear light-yellow solution) was then dried over magnesium sulfate and placed in a wash bottle. Ammonia gas was slowly bubbled through the solution for ~15 min at room temperature resulting in a slight change of color and the precipitation of a fine white crystalline solid. The solid was then removed by vacuum filtration and washed twice with 20 mL of fresh dichloroethane. The solvent collected was set aside, and the white solid was allowed to dry overnight in air yielding 2.2 g (15.6 mmol) of white crystalline powder (ammonium 5-nitrotetrazolate hemihydrate). The depleted dichloroethane was then transferred back to a wash bottle and treated with ammonia for a further 15 min. No additional solid precipitated. The remaining aqueous reaction solution from the previous extraction was then extracted with a second solution of 12 mL (18.9 mmol) of tridodecylamine in 150 mL of dichloroethane. The organic phase was once again dried, treated with ammonia gas and filtered as described above yielding 1.4 g (9.9 mmol) of ammonium 5-nitrotetrazolate hemihydrate. The portions of solid collected were combined giving a total yield of 3.6 g (25.5 mmol, 51%). Crystals suitable for X-ray diffraction were prepared by slow evaporation of a methanolic solution of **1a**. (Crystals of **1** suitable for X-ray diffraction were prepared by slow diffusion of diethyl ether into a dry acetone solution of material (**1a**) which had been stored in a desiccator for ~1 week.) mp 207 °C (decomp, DSC); IR (KBr, cm^{-1}) $\tilde{\nu}$ = 3396(m), 3179(w), 3141(w), 3044(s), 2900(m), 2856(m), 2732(w), 2080(w), 1823(wb), 1712(m), 1669(m), 1541(s), 1508(w), 1464(m), 1448(m), 1418(s), 1316(s), 1184(m), 1167(m), 1067(w), 1051(w), 1035(w), 834(m), 771(w), 736(w), 707(m), 669(m); Raman (200 mW, 25 °C, cm^{-1}) $\tilde{\nu}$ = 3063(3), 2837(1), 1875(1), 1689(1), 1555(8), 1445(5), 1421(100), 1318(6), 1185(2), 1168(4), 1071(63), 1053(21), 836(9), 775(4), 541(4), 454(3), 252(5), 197(3); 1H NMR (DMSO-d_6, 25 °C) δ 7.11 (s, NH_4^+), 3.48 (s, H_2O); ^{13}C NMR (DMSO-d_6, 25 °C) δ 169.5 (*C*5); ^{14}N NMR (DMSO-d_6, 25 °C) δ 19 (*N*2, $\nu_{1/2}$ = 430 Hz), −22 (*N*5, $\nu_{1/2}$ = 60 Hz), −62 (*N*1, $\nu_{1/2}$ = 400 Hz), −359 (NH_4^+, $\nu_{1/2}$ = 10 Hz); *m*/*z* (FAB$^-$, xenon, 6 keV, m-NBA matrix) [NT]$^-$ 114; $CH_5N_6O_{2.5}$ (141.09) calcd: C 8.5, H 3.6, N 59.6%; found: C 8.5, H 3.6, N 59.6%.

Synthesis of Hydrazinium 5-Nitrotetrazolate (2). To a suspension of 1.32 g of ammonium 5-nitrotetrazolate hemihydrate (9.4 mmol) in 3 mL of ethanol were added 0.5 mL (0.5 g, 10.0 mmol) of hydrazine hydrate. The solution was subsequently warmed to boiling with a heat gun to drive off the ammonia evolved. The resulting solution was allowed to cool to room temperature and was then refrigerated overnight. No material precipitated. The resulting yellowish solution was then divided into three 1 mL portions, each of which was evaporated to dryness individually. After removing the solvent, each portion was recrystallized from 2−3 mL of boiling ethanol. Each portion of recrystallized material was vacuum-filtered and washed twice with diethyl ether. The total combined yield of colorless plates was 0.78 g (5.3 mmol) 56%. Crystals suitable for X-ray structure determination were obtained by slow diffusion of diethyl ether into a methanol solution of **2**. mp 135 °C (DSC); IR (KBr, cm^{-1}) $\tilde{\nu}$ = 3303(s), 3250(m), 3185(m), 3079(m), 2960(m), 2864(m), 2727(m), 2654(m), 2462(w), 2079(w), 1631(m), 1597(m), 1531(s), 1507(m), 1444(m), 1420(s), 1318(s), 1175(w), 1149(m), 1117(m), 1063(w), 1044(w), 1026(w), 979(m), 838(m), 771(w), 664(m); Raman (200 mW, 25 °C, cm^{-1}) $\tilde{\nu}$ = 3090(2), 2836(2), 2462(2), 1873(2), 1633(4), 1532(6), 1446(4), 1420(100), 1316(7), 1291(1), 1177(3), 1162(5), 1122(1), 1062(58), 1046(41), 1029(5), 980(7), 840(9), 773(3), 542(3), 454(3), 258(4), 174(2), 129(3); ^{1}H NMR (DMSO-d_6, 25 °C) δ 6.71 (s, $N_2H_5^+$); ^{13}C NMR (DMSO-d_6, 25 °C) δ 169.0 (*C*5); ^{14}N NMR (DMSO-d_6, 25 °C) δ 18 (*N*2, $\nu_{1/2}$ = 900 Hz), −23 (*N*5, $\nu_{1/2}$ = 110 Hz), −59 (*N*1, $\nu_{1/2}$ = 990 Hz), −338 ($N_2H_5^+$, $\nu_{1/2}$ = 1980 Hz); *m*/*z* (FAB$^-$, xenon, 6 keV, m-NBA matrix) [NT]$^-$ 114; *m*/*z* (FAB$^+$, xenon, 6 keV, m-NBA matrix) $[N_2H_5]^+$ 33; $CH_5N_7O_2$ (147.12) calcd: C 8.2, H 3.4, N 66.7%; found: C 8.3, H 3.3, N 66.6%.

Synthesis of Guanidinium 5-Nitrotetrazolate (3). To a solution of 1.32 g of ammonium 5-nitrotetrazolate hemihydrate (9.4 mmol) in 3 mL of water were added 1.22 g (10.0 mmol) of guanidinium nitrate. The mixture was warmed with a heat gun until all solids dissolved and then allowed to cool to room temperature overnight yielding colorless crystals of guanidinium 5-nitrotetrazolate, which were vacuum-filtered and subsequently washed twice with diethyl ether. Yield 1.31 g (7.6 mmol) 81%. Crystals suitable for X-ray structure determination were obtained by slow diffusion of diethyl ether into a methanol solution of **3**. mp 212 °C (decomp., DSC); IR (KBr, cm^{-1}) $\tilde{\nu}$ = 3503(s), 3407(s), 3371(s), 3177(s), 2839(w), 2727(w), 2483(w), 2455(w), 2367(w), 2204(w), 2052(w), 1645(s), 1581(m), 1522(m), 1437(m), 1416(m), 1314(m), 1168(w), 1112(w), 1048(w), 1039(w), 1029(s), 838(m), 739(w), 664(w); Raman (200 mW, 25 °C, cm^{-1}) $\tilde{\nu}$ = 3203(1), 1643(1), 1569(3), 1541(5), 1419(100), 1317(3), 1179(3), 1051(41), 1042(32), 1016(25), 843(6), 773(1), 545(9), 455(2), 268(3), 135(7), 116(3); ^{1}H NMR (DMSO-d_6, 25 °C) δ 6.89 (s, $CH_6N_3^+$); ^{13}C NMR (DMSO-d_6, 25 °C) δ 169.3 (*C*5), 158.4 (*C*1); ^{14}N NMR (DMSO-d_6, 25 °C) δ 20 (*N*2, $\nu_{1/2}$ = 490 Hz), −23 (*N*5, $\nu_{1/2}$ = 60 Hz), −62 (*N*1, $\nu_{1/2}$ = 390 Hz), −306 $CH_6N_3^+$, $\nu_{1/2}$ = 1460); *m*/*z* (FAB$^-$, xenon, 6 keV, m-NBA matrix) [NT]$^-$ 114; *m*/*z* (FAB$^+$, xenon, 6 keV, m-NBA matrix) $[CH_6N_3]^+$ 60; $C_2H_6N_8O_2$ (174.15) calcd: C 13.8, H 3.5, N 64.4%; found: C 13.8, H 3.5, N 64.4%.

Synthesis of Aminoguanidinium 5-Nitrotetrazolate (4). A suspension of 4.23 g (30.0 mmol) of ammonium 5-nitrotetrazolate hemihydrate and 5.67 g (30.0 mmol) of aminoguanidinium hydrogen carbonate in 50 mL of ethanol was heated to reflux under dry N_2 overnight. The clear, slightly yellow solution was allowed to cool slowly to room temperature under dry N_2 resulting in the precipitation of 2.72 g (14.4 mmol) of fine white solid aminoguanidinium 5-nitrotetrazolate. The precipitated material was filtered and washed with cold ethanol and then twice with diethyl ether. The ethanol was retained and reduced in volume on a rotary evaporator

until further material precipitated. A second portion of 1.58 g (8.4 mmol) of **4** was collected, and the remaining ethanol solution was evaporated to dryness. The remaining white material was recrystallized once from ethanol and then washed with ether yielding a further 0.92 g (4.9 mmol) of **4**. The total yield of **4** is 5.2 g (27.5 mmol, 92%). Crystals suitable for X-ray structure determination were obtained by slow diffusion of diethyl ether into a methanol solution of **4**. mp 147 °C (DSC); IR (KBr, cm^{-1}) $\tilde{\nu}$ = 3412(s), 3360(m), 3336(m), 3246(m), 3154(m), 3074(m), 2848(w), 2735(w), 2634(w), 2459(w), 2191(w), 2071(w), 1661(s), 1637(m), 1543(m), 1533(m), 1503(w), 1446(m), 1422(m), 1319(m), 1197(w), 1175(w), 1158(w), 1064(w), 1027(w), 940(m), 835(m), 757(w), 720(w), 668(w), 618(w), 583(w); Raman (200 mW, 25 °C, cm^{-1}) $\tilde{\nu}$ = 3293(2), 1869(1), 1674(1), 1630(2), 1533(7), 1490(2), 1422(100), 1319(5), 1285(1), 1204(2), 1177(3), 1159(4), 1063(45), 1041(44), 959(7), 838(8), 773(3), 626(3), 539(3), 497(4), 450(3), 348(4), 261(2), 243(4), 206(3), 133(7); ^{1}H NMR (DMSO-d_6, 25 °C) δ 8.53 (s, -N6*H*), 7.23 (broad s, -N8H_2), 6.71 (broad s, -N7H_2), 4.66 (s, -N9H_2); ^{13}C NMR (DMSO-d_6, 25 °C) δ 169.3 (*C*5), 159.3 (*C*1); ^{14}N NMR (DMSO-d_6, 25 °C) δ 15 (*N*2, $\nu_{1/2}$ = 720 Hz), −23 (*N*5, $\nu_{1/2}$ = 70 Hz), −62 (*N*1, $\nu_{1/2}$ = 460 Hz), −306 ($CH_7N_4^+$, $\nu_{1/2}$ = 2000 Hz); *m*/*z* (FAB$^-$, xenon, 6 keV, m-NBA matrix) [NT]$^-$ 114; *m*/*z* (FAB$^+$, xenon, 6 keV, m-NBA matrix) $[CH_7N_4]^+$ 75; $C_2H_7N_9O_2$ (189.14) calcd: C 12.7, H 3.7, N 66.7%; found: C 12.8, H 3.7, N 66.4%.

Synthesis of Diaminoguanidinium 5-Nitrotetrazolate (5). A suspension of 0.35 g (2.5 mmol) of ammonium 5-nitrotetrazolate hemihydrate, 0.265 g (2.5 mmol) of sodium carbonate and 0.468 g (2.5 mmol) of 1-amino-3-ammonioguanidnium sulfate were suspended in ∼20 mL of ethanol. The mixture was refluxed under a flow of N_2 while stirring overnight. The resulting white suspension was then cooled under N_2 and filtered yielding (after drying in an oven at 100 °C for 15 min.) 0.33 g of fine white powder solids (Na_2SO_4). The remaining clear, slightly yellow solution was then reduced in volume to ∼2 mL using a rotary evaporator (bath temp 50 °C). A white solid crystallized immediately upon removal from the rotary evaporator. ∼2 mL of ethanol were then added, and the mixture was subsequently heated until all material had dissolved. After cooling, the white powder solid that precipitated was filtered and washed with ethanol (0.25 g, 1.2 mmol). Some material redissolved on washing and the filtrate was thus reduced in volume to ∼2 mL, and diethyl ether was diffused into the solution overnight resulting in the formation crystalline material. The solution was decanted off, and the remaining solids were allowed to dry in air for ∼15 min. A 0.11 g (0.54 mmol) quantity of additional material was recovered. Total yield 0.36 g (1.76 mmol, 71%). Crystals suitable for X-ray structure determination were obtained by slow diffusion of diethyl ether into a methanol solution of **5**. mp 108 °C (DSC); IR (KBr, cm^{-1}) $\tilde{\nu}$ = 3412(s), 3349(s), 3295(s), 3233(s), 3196(s), 2843(w), 2455(w), 2207(w), 2071(w), 1663(s), 1633(m), 1532(s), 1503(m), 1441(m), 1417(s), 1373(m), 1316(m), 1187(m), 1176(m), 1055(w), 1029(w), 991(m), 941(m), 836(m), 771(w), 666(m), 580(w); Raman (200 mW, 25 °C, cm^{-1}) $\tilde{\nu}$ = 3300(3), 2987(5), 2451(1), 1867(1), 1675(3), 1618(3), 1538(10), 1444(17), 1414(100), 1317(7), 1182(10), 1057(54), 1041(79), 1014(8), 929(11), 839(14), 773(5), 732(2), 659(2), 545(6), 451(3), 370(4), 271(5), 259(6), 242(5), 186(3), 133(5); ^{1}H NMR (DMSO-d_6, 25 °C) δ 8.52 (s, 2H, -N6/8*H*), 7.11 (s, -N7H_2), 4.56 (s, 4H, -N9/11H_2); ^{13}C NMR (DMSO-d_6, 25 °C) δ 169.3 (*C*5), 160.3 (*C*1); ^{14}N NMR (DMSO-d_6, 25 °C) δ 16 (*N*2, $\nu_{1/2}$ = 620 Hz), −23 (*N*5, $\nu_{1/2}$ = 70 Hz), −62 (*N*1, $\nu_{1/2}$ = 510 Hz); *m*/*z* (FAB$^-$, xenon, 6 keV, m-NBA matrix) [NT]$^-$ 114; *m*/*z*(FAB$^+$, xenon, 6 keV, m-NBA matrix) $[CH_8N_5]^+$ 90; $C_2H_8N_{10}O_2$ (204.18) calcd: C 11.8, H 4.0, N 68.6%; found: C 11.8, H 3.8, N 68.7%.

Synthesis of Triaminoguanidinium 5-Nitrotetrazolate Monohydrate (6a). To a solution of 1.41 g (10.0 mmol) of ammonium 5-nitrotetrazolate hemihydrate in a mixture of 4 mL of water and 6 mL of methanol in a pear shaped flask were added 1.57 g (5.0 mmol) of barium hydroxide octahydrate. The mixture was heated with a heat gun until all solids had dissolved. The volume was then reduced to ∼5 mL on a rotary evaporator with heating to remove as much ammonia as possible. The pH was subsequently checked (7−8). Meanwhile, 1.62 g (5.0 mmol) of triaminoguanidinium hemisulfate dihydrate were dissolved in ∼5 mL of deionized water. After cooling, the barium 5-nitrotetrazolate solution was added dropwise resulting in the formation of a white precipitate. The solution was stirred for ∼1 h and then filtered. The solvent from the resulting clear orange solution was then removed on a rotary evaporator, yielding an orange oil. The oil was subsequently redissolved in ∼10 mL of acetonitrile and filtered. The volume of the acetonitrile solution was then reduced to ∼5 mL, and the solution was cooled to 4 °C overnight yielding 1.2 g (5.1 mmol, 50%) of colorless crystals. Crystals suitable for X-ray structure determination were obtained by slow diffusion of diethyl ether into an acetonitrile solution of **6a**. mp 63 °C (DSC); IR (KBr, cm^{-1}) $\tilde{\nu}$ = 3339(s), 3225(sb), 2844(w), 2726(w), 2452(w), 2198(w), 2067(w), 1988(w), 1681(s) 1609(w), 1551(m), 1503(w), 1440(m), 1414(m), 1344(m), 1315(m), 1178(m), 1162(w), 1132(m), 1054(w), 1039(w), 943(m), 833(m), 667(w); Raman (200 mW, 25 °C, cm^{-1}) $\tilde{\nu}$ = 3340(1), 3240(3), 2454(0), 1861(1), 1685(2), 1645(1), 1553(3), 1536(6), 1441(4), 1416(100), 1341(3), 1318(4), 1198(1), 1179(2), 1163(4), 1137(3), 1056(52), 1040(35), 1028(11), 884(8), 838(7), 772(3), 637(2), 537(5), 447(2), 399(2), 257(5), 215(4), 140(5); ^{1}H NMR (DMSO-d_6, 25 °C) δ 8.57 (s, 3H, -N*H*), 4.46 (s, 6H, -NH_2), 3.49 (s, H_2O); ^{13}C NMR (DMSO-d_6, 25 °C) δ 169.1 (*C*5), 159.6 (*C*1); ^{14}N NMR (DMSO-d_6, 25 °C) δ 18 (*N*2, $\nu_{1/2}$ = 780 Hz), −23 (*N*5, $\nu_{1/2}$ = 90 Hz), −61 (*N*1, $\nu_{1/2}$ = 670 Hz); *m*/*z* (FAB$^-$, xenon, 6 keV, m-NBA matrix) [NT]$^-$ 114;*m*/*z* (FAB$^+$, xenon, 6 keV, m-NBA matrix) $[CH_9N_6]^+$ 105; $C_2H_{11}N_{11}O_3$ (237.18) calcd: C 10.1, H 4.7, N 65.0%; found: C 10.3, H 4.5, N 64.9%.

Synthesis of Triaminoguanidinium 5-Nitrotetrazolate (6). Finely powdered **6a** was stored in a desiccator over phosphorus pentoxide for 1 week. Crystals suitable for X-ray structure determination were obtained by slow diffusion of diethyl ether into an anhydrous acetonitrile solution of **6**. mp 96 °C (DSC); IR (KBr, cm^{-1}) $\tilde{\nu}$ = 3369(m), 3334(s), 3295(s), 3260(m), 3197(m), 3127(m), 2839(w), 2721(w), 2451(w), 2212(w), 1685(s), 1590(m), 1536(s), 1507(w), 1438(m), 1414(m), 1375(m), 1311(m), 1212(w), 1180(w), 1143(m), 1132(m), 1039(m), 1028(m), 985(m), 927(m), 835(m), 740(w), 666(w), 632(w), 579(w); Raman (200 mW, 25 °C, cm^{-1}) $\tilde{\nu}$ = 3294(3), 2986(5), 1688(4), 1638(2), 1534(9), 1439(4), 1415(100), 1316(7), 1204(2), 1181(3), 1153(6), 1054(43), 1042(30), 1029(12), 886(10), 839(12), 773(4), 639(2), 535(4), 447(4), 406(7), 330(3), 254(8), 197(6); $C_2H_9N_{11}O_2$ (219.20) calcd: C 11.0, H 4.1, N 70.3%; found: C 11.0, H 4.3, N 70.4%.

X-ray Crystallography. Crystals were obtained as described above. The X-ray crystallographic data for **1**, **2**, and **3** were collected on an Enraf-Nonius Kappa CCD diffractometer. Data sets for **1a**, **5**, **6a**, and **6** were collected on an Oxford Diffraction Xcalibur 3 diffractometer equipped with a CCD detector. Data for **4** were collected on a STOE IPDS diffractometer. All data were collected using graphite-monochromated Mo Kα radiation (λ = 0.71073 Å). No absorption corrections were applied to data sets collected for **1**, **1a**, **2**, **3**, **4**, **5**, or **6a**. A multiscan semiempirical absorption

Table 1. Crystallographic Data and Structure Determination Details for Compounds **1**−**6**

	1	**1a**	**2**	**3**	**4**	**5**	**6**	**6a**
weight (g/mol)	132.1	141.11	147.12	174.15	189.17	204.18	219.20	237.22
crystal system	monoclinic	monoclinic	monoclinic	monoclinic	monoclinic	monoclinic	orthorhombic	triclinic
space group	$P2_1/c$	$C2/c$	$P2_1/c$	$C2/c$	$P2_1/n$	$P2_1$	$P2_12_12_1$	$P\bar{1}$
a (Å)	4.8436(2)	10.4860(13)	8.0124(3)	9.8240(3)	6.9447(5)	6.8162(9)	4.4024(4)	6.9805(9)
b (Å)	13.7981(6)	8.1461(10)	10.3237(5)	11.7601(4)	6.3716(6)	7.3468(10)	9.5261(7)	8.1249(9)
c (Å)	8.0853(4)	13.8381(17)	7.1531(3)	6.8736(2)	17.3196(12)	17.001(2)	21.6851(14)	9.1040(10)
α (°)	90	90	90	90	90	90	90	88.480(9)
β (°)	97.2558(17)	104.207(11)	106.186(3)	117.6043(13)	99.152(8)	92.774(11)	90	74.880(10)
γ (°)	90	90	90	90	90	90	90	81.314(10)
V (Å^3)	536.03(4)	1145.9(3)	568.23(4)	703.72(4)	756.62(10)	850.4(2)	909.42(12)	492.70(10)
Z	4	4	4	4	4	4	4	2
ρ_{calcd} (g/cm^3)	1.637	1.636	1.72	1.644	1.661	1.595	1.601	1.599
μ (mm^{-1})	0.147	0.149	0.153	0.141	0.142	0.136	0.136	0.139
λ (Mo Kα, Å)	0.71073	0.71069	0.71073	0.71073	0.71073	0.71069	0.71069	0.71069
T (K)	200(2)	140(2)	200(2)	200(2)	200(2)	200(2)	100(2)	140(2)
reflns collected	6065	2875	6560	5932	6344	6000	11757	5044
ind. reflections	1229	1120	1294	804	1492	2645	1579	1926
R_{int}	0.1018	0.0292	0.0806	0.0922	0.0493	0.0516	0.0984	0.0366
obs. reflections	959	1001	997	738	1721	1711	921	1749
F(000)	272	584	304	360	392	424	456	248
R_1[a]	0.0559	0.0329	0.0576	0.0395	0.0499	0.0665	0.0417	0.0406
wR_2[b]	0.1144	0.088	0.1124	0.1039	0.0872	0.1091	0.0812	0.0963
weighting scheme[c]	0.0641, 0.0000	0.0499, 0.6428	0.0594, 0.0801	0.0545, 0.2774	0.0544, 0.0000	0.0327, 0.0000	0.0301, 0.0000	0.04010, 0.1780
GOF	1.057	1.05	1.047	1.08	1.131	1.046	0.99	1.093
no. of parameters	99	107	112	69	146	301	172	189

[a] $R_1 = \sum||F_o| - |F_c||/\sum|F_o|$. [b] $R_w = [\sum(F_o^2 - F_c^2)/\sum w(F_o)^2]^{1/2}$. [c] $w = [\sigma_c^2(F_o^2) + (xP)^2 + yP]^{-1}$, $P = (F_o^2 - 2F_c^2)/3$.

Table 2. Calculated and Measured IR and Raman Frequencies, Intensities (IR), and Activities (Raman) for the 5-Nitrotetrazolate (NT) Anion

	ν_{calc} (cm^{-1})[a]	ν_{meas} (cm^{-1})[b] (IR/Raman)	IR intensity (calc/obs)[c]	Raman activity(calc/obs)[d]	mode assignment[e]
1	1538	1533(6)/1538(8)	74.1/s	3.8/7.3	$\nu_{asymm}(NO_2)$
2	1396	1442(5)/1443(3)	19.5/s	0.18/6	ν_{asymm}(N1−C5−N4)
3	1383	1417(3)/1418(4)	100/vs	100/100	$\nu_{symm}(NO_2) + \nu_{symm}$(N1−C5−N4), "in phase"
4	1294	1316(3)/1317(2)	12.6/s	0.4/5.6	$\nu_{symm}(NO_2) + \nu_{symm}$(N1−C5−N4), "out of phase"
5	1182	1181(9)/1180(3)	2.0/m	2.6/3.7	ν_{asymm}(Tetrazole)
6	1163	1158(9)/1164(7)	19.7/m	4.0/4.6	ν_{symm}(Tetrazole) + $\nu_{symm}(NO_2)$, "in phase"
7	1024	1058(7)/1059(7)	0.2/w	8.0/50.9	δ(N1−C5−N4) + $\nu_{symm}(NO_2)$, "in phase"
8	1018	1042(5)/1044(5)	1.2/vw	3.8/40.3	δ_{asymm}(Tetrazole)
9	966	1029(3)/1030(6)	19.0/w	64.4/7.6	ν(N2−N3) + δ_{symm}(Tetrazole), "out of phase"
10	821	836(2)/839(3)	14.4/s	5.0/9.3	$\delta(NO_2) + \delta$(N1−C5−N4), "in of phase"
11	763	765(13)/773(1)	2.4/vw	0.8/3.3	$\gamma(NO_2) + \gamma$(N1−C5−N4), "out of phase"
12	718	725(13)/730(11)	0/vw	0.001/1.1	γ(Tetrazole) "in phase"
13	664	667(2)/669(3)	3.3/w	0.2/1	γ(Tetrazole) "out of phase"
14	522	n.o./540(4)	0.02/n.o.	2.3/4.9	$\omega(NO_2) + \omega$(Tetrazole), "out of phase"
15	439	n.o./451(4)	0.2/n.o.	1.8/2.9	ν(C5−N5) + $\delta(NO_2)$
16	242	n.o./245(3)	0.2/n.o.	0.3/3.4	$\omega(NO_2) + \omega$(Tetrazole), "in phase"
17	218	n.o./208(8)	1.9/n.o.	0.3/1.3	γ(N1−C5−N4)
18	57	n.o./62(5)	0/n.o.	0.03/1	τ(C5−N5)

[a] Calculated frequencies; scaled by 0.9613.[28] [b] Measured frequencies; average values from IR and Raman spectra of compounds **1**−**6**, with standard deviations shown in parentheses; n.o. not observed. [c] Calculated intensities; percentages of the most intense signal; qualitative observed intensities; n.o. not observed. [d] Activities as percentage of the most intense signal; measured intensities are average values from **1**−**6**. [e] Approximate description of vibrational modes; ν, stretching, δ, in-plane bending, γ, out-of-plane bending, ω, in plane rocking, τ, torsion; asymm, asymmetric and symm symmetric; for atom numbering see X-ray section.

correction was applied to data collected for **6** using the ABSPACK[23] software supplied by Oxford Diffraction. All structures were solved by direct methods (SHELXS-97 and SIR97)[24,25] and refined by means of full-matrix least-squares procedures using SHELXL-97.[24] In the cases of **5** and **6**, which crystallize in the noncentrosymmetric space group $P2_1$ and $P2_12_12_1$, respectively, the Friedel pairs in these data sets were averaged because no meaningful information about absolute structure configuration could be obtained from anomalous scattering effects. All non-hydrogen atoms were refined anisotropically. All hydrogen atoms were located from difference Fourier electron-density maps. For all structures except **5** all hydrogen atoms were refined isotropically. In the case of **5**, the hydrogen atoms refined with fixed isotropic temperature factors with the value of 1.2 *B*eq. Crystallographic data are summarized in Table 1. Selected bond lengths and angles are reported in Table 3 and hydrogen-bonding geometries in Supporting Information, Table 1. Further information concerning the crystal-structure determinations (excluding structure factors) in CIF format is available in the Supporting Information.

(23) *ABSPACK, CrysAlis CCD and CrysAlis RED*, 1.171; Oxford Diffraction Ltd: Abingdon, Oxfordshire, England, 2006.

(24) Sheldrick, G. M. *Programs for Crystal Structure Analysis* (Release 97−2); Goettingen, Germany, 1998.

(25) Altomare, A.; Burla, M. C.; Camalli, M.; Cascarano, G. L.; Giacovazzo, C.; Guagliardi, A.; Moliterni, A. G. G.; Polidori, G.; Spagna, R. *J. Appl. Crystallogr.* **1999**, *32*, 115–119.

Table 3. Selected Bond Lengths (Å), Angles (°), and Torsion Angles (°) in Compounds **1**−**6**[a]

	1	1a	2	3	4	5[b]	6	6a
				Bond Lengths				
C5−N1	1.3219(15)	1.3215(17)	1.3232(18)	1.3261(11)	1.3220(16)	1.314(5)/1.317(5)	1.330(3)	1.3260(19)
C5−N4	1.3216(16)	1.3236(17)	1.3185(17)	1.3261(11)	1.3112(18)	1.313(5)/1.319(5)	1.332(3)	1.3275(19)
C5−N5	1.4398(17)	1.4515(17)	1.4414(19)	1.4410(19)	1.4437(16)	1.453(6)/1.452(5)	1.445(3)	1.448(2)
N1−N2	1.3341(17)	1.3422(16)	1.3389(17)	1.3366(13)	1.3387(16)	1.342(5)/1.341(5)	1.350(3)	1.3413(19)
N2−N3	1.3256(15)	1.3278(16)	1.3202(18)	1.3263(19)	1.3167(18)	1.323(5)/1.330(5)	1.341(3)	1.3363(19)
N3−N4	1.3391(16)	1.3450(16)	1.3419(17)	1.3366(13)	1.3378(16)	1.339(5)/1.340(5)	1.351(3)	1.336(2)
N5−O1	1.2199(15)	1.2265(15)	1.2271(16)	1.2254(10)	1.2218(15)	1.218(5)/1.224(4)	1.235(3)	1.2241(18)
N5−O2	1.2297(14)	1.2306(15)	1.2265(17)	1.2254(10)	1.2190(15)	1.226(4)/1.226(4)	1.236(3)	1.2264(18)
				Bond Angles				
N1−C5−N4	114.10(11)	114.94(11)	114.75(13)	115.14(12)	114.75(11)	115.3(4)/115.4(4)	114.9(2)	114.75(14)
N1−C5−N5	123.15(11)	123.17(12)	122.50(12)	122.43(6)	123.23(12)	122.0(4)/122.7(3)	122.7(2)	123.27(13)
N4−C5−N5	122.75(13)	121.87(11)	122.76(12)	122.43(6)	122.02(11)	122.7(4)/121.9(3)	122.3(3)	121.96(13)
C5−N1−N2	103.68(10)	102.97(11)	103.03(11)	102.47(8)	102.78(11)	102.7(3)/103.0(3)	103.1(2)	103.05(12)
N3−N2−N1	109.31(11)	109.67(11)	109.53(11)	109.96(6)	109.67(11)	109.5(3)/109.1(3)	109.3(2)	109.36(13)
N2−N3−N4	109.70(11)	109.57(10)	109.91(11)	109.96(6)	109.67(11)	109.6(3)/110.0(3)	109.7(2)	109.87(12)
C5−N4−N3	103.21(11)	102.84(10)	102.78(11)	102.47(8)	103.13(11)	102.9(3)/102.5(3)	102.9(2)	102.97(12)
O1−N5−O2	125.15(12)	125.23(12)	124.50(14)	124.24(13)	124.76(12)	126.2(4)/124.4(4)	124.4(2)	124.42(15)
O1−N5−C5	117.89(12)	117.55(11)	117.74(12)	117.88(7)	117.14(12)	118.1(4)/118.1(3)	118.4(2)	117.34(14)
O2−N5−C5	116.96(12)	117.20(11)	117.76(13)	117.88(7)	118.10(11)	115.7(4)/117.5(4)	117.2(2)	118.23(13)
				Torsion Angles				
O1−N5−C5−N4	176.47(11)	−169.04(12)	175.48(12)	−177.22(7)	−172.04(12)	−176.8(4)/178.7(4)	−176.2(2)	−176.71(14)
O2−N5−C5−N4	−3.95(16)	9.59(18)	−4.86(19)	2.78(7)	8.23(18)	3.7(6)/0.6(5)	3.7(4)	1.9(2)
O1−N5−C5−N1	−3.20(16)	9.61(18)	−4.28(19)	2.78(7)	7.49(18)	2.0(6)/1.1(5)	3.3(4)	2.5(2)
O2−N5−C5−N1	176.38(11)	−171.75(12)	175.38(12)	−177.22(7)	−172.23(13)	−177.5(4)/−177.0(4)	−176.7(3)	−178.96(14)

[a] Bond lengths, angles and torsion angles from the NT anion. [b] Parameters for both anions in the asymmetric unit of **5** are shown (A/B).

Computational Methods. All quantum chemical calculations were carried out with the Gaussian 03W software package.[26] Vibrational (IR and Raman) frequencies of the 5-nitrotetrazolate anion were calculated using Becke's B3 three parameter hybrid function with an LYP correlation function (B3LYP)[27] and were scaled by a factor of 0.9614 as described by Radom et al.[28] Electronic energies for all cations and the 5-nitrotetrazolate anion were calculated using Møller−Plesset perturbation theory truncated at the second order (MP2)[29] and were used unscaled. The results of the MP2 electronic energy calculations are tabulated in Supporting Information, Table 9. For all atoms in all calculations, the correlation consistent polarized double-ζ basis set cc-pVDZ was used.[30,31]

Scheme 1. Synthesis of NT Salts by Silver Salt Metathesis Reactions

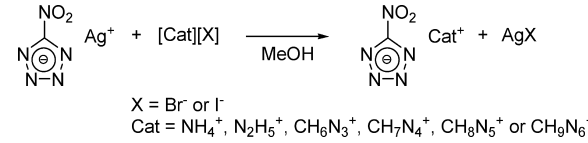

Results and Discussion

Synthesis. **1a** was prepared by a slightly modified literature method. However, Lee et al. describe the material obtained as compound **1**.[22] In our hands, the preparation loosely described by Lee et al. and described in detail here yielded exclusively **1a** as identified by elemental analysis and X-ray structure determination. Lee et al. reported isolated yields of >70%, and we normally obtained ∼50% yields and upon scale-up (quadruple the procedure reported here) we obtained just over 60% yield of **1a**. In addition, Lee et al. also reported several properties of the bulk material generated (density, heat of formation, sensitivity to impact, friction and electrostatic discharge, and predicted energetic performance), which we found either to be in reasonable agreement with values measured for **1a** (sensitivities and density) or values calculated based on the assumption that the material generated was **1** (heat of formation, predicted energetic performance). Therefore, we suggest that the material isolated by Lee et al. was probably **1a** in slightly lower yield than reported.

Initially, the compounds **1**−**6** were prepared by metathesis of silver 5-nitrotetrazolate with the corresponding bromide or iodide salts as shown in Scheme 1. However, the synthesis of energetic salts for study using silver 5-nitrotetrazolate as the 5-nitrotetrazole transfer reagent was unsuitable for several reasons. First, silver 5-nitrotetrazolate is extremely sensitive to impact, friction, and electrostatic discharge; manipulation

(26) Frisch, M. J.; Trucks, G. W.; Schlegel, H. B.; Scuseria, G. E.; Robb, M. A.; Cheeseman, J. R.; Montgomery, J. J. A.; Vreven, T.; Kudin, K. N.; Burant, J. C.; Millam, J. M.; Iyengar, S. S.; Tomasi, J.; Barone, V.; Mennucci, B.; Cossi, M.; Scalmani, G.; Rega, N.; Petersson, G. A.; Nakatsuji, H.; Hada, M.; Ehara, M.; Toyota, K.; Fukuda, R.; Hasegawa, J.; Ishida, M.; Nakajima, T.; Honda, Y.; Kitao, O.; Nakai, H.; Klene, M.; Li, X.; Knox, J. E.; Hratchian, H. P.; Cross, J. B.; Bakken, V.; Adamo, C.; Jaramillo, J.; Gomperts, R.; Stratmann, R. E.; Yazyev, O.; Austin, A. J.; Cammi, R.; Pomelli, C.; Ochterski, J. W.; Ayala, P. Y.; Morokuma, K.; Voth, G. A.; Salvador, P.; Dannenberg, J. J.; Zakrzewski, V. G.; Dapprich, S.; Daniels, A. D.; Strain, M. C.; Farkas, O.; Malick, D. K.; Rabuck, A. D.; Raghavachari, K.; Foresman, J. B.; Ortiz, J. V.; Cui, Q.; Baboul, A. G.; Clifford, S.; Cioslowski, J.; Stefanov, B. B.; Liu, G.; Liashenko, A.; Piskorz, P.; Komaromi, I.; Martin, R. L.; Fox, D. J.; Keith, T.; Al-Laham, M. A.; Peng, C. Y.; Nanayakkara, A.; Challacombe, M.; Gill, P. M. W.; Johnson, B.; Chen, W.; Wong, M. W.; Gonzalez, C.; Pople, J. A. *Gaussian 03*, Revision C.02; Gaussian, Inc.: Wallingford, CT, 2004.
(27) Miehlich, B.; Savin, A.; Stoll, H.; Preuss, H. *Chem. Phys. Lett.* **1989**, *157*, 200–206.
(28) Scott, A. P.; Radom, L. *J. Phys. Chem.* **1996**, *100*, 16502–16513.
(29) Pople, J. A.; Seeger, R.; Krishnan, R. *Int. J. Quantum Chem., Symp.* **1977**, *11*, 149–163.
(30) Rick, A. K.; Dunning, T. H.; Robert, J. H. *J. Chem. Phys.* **1992**, *96*, 6796–6806.
(31) Kirk, A. P.; David, E. W.; Dunning, T. H. *J. Chem. Phys.* **1994**, *100*, 7410–7415.

Scheme 2. Applied and Proposed Scalable Syntheses of Nitrogen-Rich NT Salts from **1a**

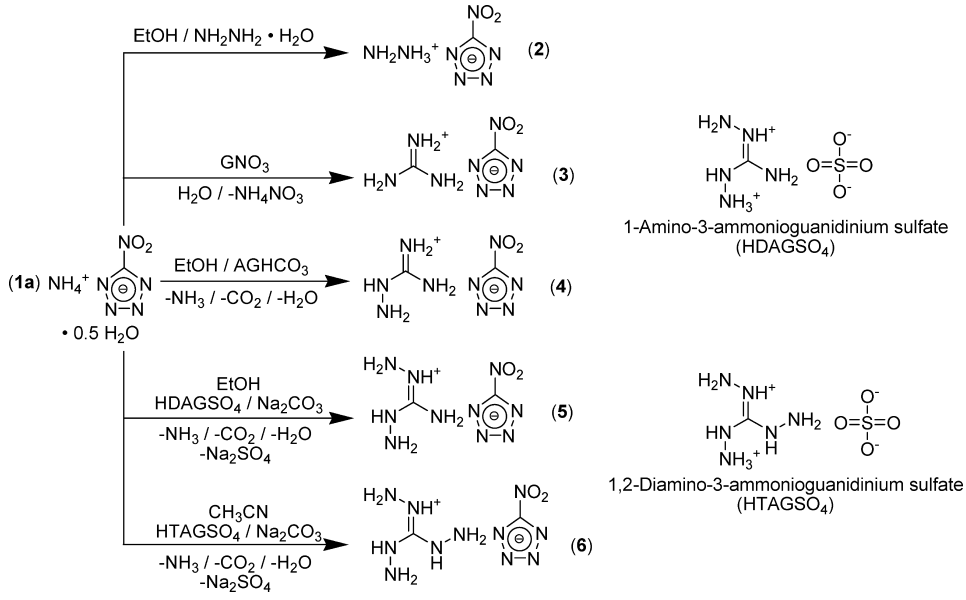

of it on a small scale (250−500 mg) requires extreme caution, and large scale (>1 g) manipulation of dry material is not advisable. Second, silver salts tend to be reduced by aminated guanidines and hydrazines to elemental silver. Therefore, even with short reaction times substantial decomposition of hydrazine and amino-, diamino- and triaminoguanidine moieties is observed.

It is also foreseeable to use 5-nitrotetrazole itself as the transfer reagent. However the free-acid 5-nitrotetrazole is reported to be both significantly friction and impact sensitive as well as hydroscopic and is, therefore, not suitable for larger scale manipulation. Therefore, **1a**, generated as discussed above, was used as a starting material. To generate compounds **2**−**4**, free bases (hydrazine hydrate and guanidine) and hydrogen carbonates (aminoguanidinium hydrogen carbonate, $AGHCO_3$) were combined with **1a** under loss of ammonia and, in the case of compound **4**, carbon dioxide. In practice, compound **3** crystallizes preferentially from a warm aqueous mixture of **1a** and guanidinium nitrate (GNO_3) and is thus most easily generated by this method. Compounds **5** and **6** can be generated using barium 5-nitrotetrazolate and the corresponding aminated guanidinium hemisulfate. However, this method is also undesirable because barium nitrotetrazolate is a sensitive explosive material which forms with variable hydration, and diamino- and triaminoguanidinium hemisulfates are not conveniently prepared on a laboratory or larger scale.[32] So, compound **5** was generated from **1a**, sodium carbonate, and 1-amino-3-ammonioguanidinium sulfate, under loss of ammonia, carbon dioxide, and sodium sulfate. A similar synthesis should be possible for **6** from 1,2-diamino-3-ammonioguanidinium sulfate and **1a**, as suggested in Scheme 2, but has not yet been applied. Methods suitable for scale-up are shown in Scheme 2 and all but that for the sensitive explosive materials **2** and **6** have been applied on at least a ∼5 g scale in our laboratories.

(32) Stierstorfer, J. Unpublished Results. Diploma, LMU, Munich, 2006.

Vibrational Spectroscopy. All salts were qualitatively identified by vibrational spectroscopy (infrared and Raman). Each compound should show a characteristic set of vibrations for both cation and anion. The vibrations associated with the cations are well-known and readily identified in the spectra of compounds **1**−**6**. The characteristic vibrations of the NT anion are either incompletely described in the literature in the case of the IR absorptions or wholly unknown in the case of the Raman bands. Therefore, to establish a characteristic set of vibrations for the NT anion, the vibrational frequencies and associated intensities and activities for the NT anion were calculated by quantum chemical methods, as described above. In addition to establishing a characteristic set of bands in the vibrational spectra of compounds **1**−**6**, quantum chemical calculations also facilitate the assignment of bands observed in the experimental spectra to individual and coupled vibrational modes, which can in turn be used to derive structural information about the NT anion and its surroundings in the solid state.

The scaled, calculated IR and Raman frequencies, calculated IR intensities, and Raman activities are summarized in Table 2, along with average measured frequencies, qualitative IR intensities, and averaged Raman activities (quantitative) from the vibrational spectra of **1**−**6**. The experimentally observed vibrations were thus assigned by comparison to the computed vibrational energies and are also tabulated in Table 2. The characteristic set of IR and Raman bands observed for the NT anion is thus established as listed in Table 2.

Remarkably, all 18 frequencies obtained from the computational results were observed in the vibrational spectra of compounds **1**−**6** with reasonably good agreement between the observed and calculated frequencies. The largest differences between calculated and observed frequencies were for those vibrations involving deformation of the tetrazole ring (vibrations 2−4 and 7−8). The scaled values for the energies of this type of vibration are always underestimated, which

is consistent with the greater rigidity of the tetrazole moiety in the solid state. Also of note is that the observed frequencies assigned to the NT anions in the vibrational spectra of **1**−**6** occur at fairly consistent energies as indicated by the reasonably narrow range of standard deviations observed for the average experimental frequencies (maximum 13 cm^{-1}). Although, because of differences in anion surroundings in the solid-state, some variation is observed in the experimental frequencies, as can been seen from the tabulated IR and Raman bands in the Experimental Section; from the IR and Raman data it is expected that the observed geometry of the NT anion should be practically identical in all compounds in this study. This prediction is confirmed by X-ray crystallography (see Table 3).

The cations in salts **1**−**6** display well-known sets of vibrations in the IR and Raman spectra. All salts show a set of strong absorptions in the IR and weak bands in the Raman spectra between 3500−2800 cm^{-1} corresponding to N−H stretching modes. N−H deformation vibrations are observed in their expected ranges as intense bands in the IR and weak bands in the Raman (1490−1390 cm^{-1} for **1** and 1700−1500 cm^{-1} for **2**−**6**). In the case of **3**−**6**, the N−H deformation vibrations are strongly coupled to the C═N stretching modes, increasing both IR and Raman intensities. Additionally, in **2** and **4**−**6**, an N−N stretching band is observed between 800−1000 cm^{-1} in both IR and Raman spectra.[33]

NMR Spectroscopy. All salts were characterized by ^{1}H, ^{13}C, and ^{14}N NMR spectroscopy, and the recorded shifts are listed in the experimental section. The NMR shifts corresponding to the cations in this study are in perfect agreement with previously recorded shifts for the appropriate cations.[34–36] The ^{13}C NMR resonance observed for C5 of the NT anion is found between 169.0 and 169.5 ppm, which is consistent both with previous reports[6,8,18–20,37,38] and with other known tetrazolate anions with electron withdrawing substituents at the 5 position of the tetrazole ring.[35] Interestingly, in the ^{14}N NMR spectra of **1**−**6** signals corresponding to all three chemically inequivalent nitrogen atoms in the NT anion are observed. The sharpest of the resonances, corresponding to the nitro group nitrogen, N5, is observed around −23 ppm with a line width between 60 and 110 Hz. The remaining two resonances are much broader (<990 Hz) but no less characteristic and are observed at around 20 ppm (N2/3) and −60 ppm (N1/4). The observation and shifts of resonances for the tetrazole ring nitrogen atoms in the ^{14}N spectra of **1**−**6** are consistent with those recorded for 5-trifluoromethyltetrazolate salts.[35] The ^{14}N NMR spectrum of **3** is shown in Figure 1.

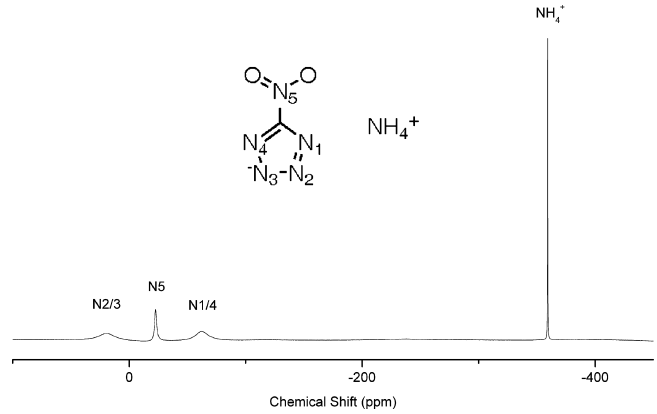

Figure 1. ^{14}Nitrogen NMR spectrum of **1a**.

X-ray Structures. Compounds **1**−**6** have been characterized by X-ray structure determination. Crystallographic data and structure determination details are presented in Table 1. Selected interatomic distances and angles are shown in Table 3. Additionally, hydrogen bond parameters are tabulated in the Supporting Information, Table 1. Compounds **1**−**5** crystallize in a variety ($P2_1/c$, $C2/c$, $P2_1/n$ and $P2_1$) of monoclinic space groups whereas **6** crystallizes in the orthorhombic space group $P2_12_12_1$ and **6a** crystallizes in triclinic $P\bar{1}$. From the unit cell parameters, no close relationships in packing may be deduced (no similar unit-cell parameters in structures with the same space groups). With the exception of **3**, which crystallizes in a layer structure similar to that of guanidinium nitrate, all other compounds crystallize as complex, three-dimensional hydrogen bonded networks of cations and anions. Lastly, extensive discussion of the hydrates **1a** and **6a** is omitted, although structural information for both compounds is provided in the Supporting Information.

The nitrogen-rich cations employed in this study are all the subject of many X-ray studies and are therefore structurally well characterized.[34–36,39–42] As suggested by vibrational spectroscopy, the NT anions in **1**−**6** are, within the limits of structure determination precision, nearly identical. From Table 3, it is also evident that the NT anion has the same geometry as was identified in previous structure determinations of NT containing salts.[20,37,43–47] The geometry of the

(33) Colthup, N. B.; Daly, L. H.; Wiberley, S. E. *Introduction to infrared and Raman spectroscopy*, 3rd ed.; Academic Press: Boston, 1990.
(34) Goebel, M.; Klapötke, T. M. *Z. Anorg. Allg. Chem.* **2007**, *633*, 1006–1017.
(35) Bernhardt, S. , Crawford, M.-J. , Klapötke, T. M. , Radies, H. *Proceedings of The 10th New Trends in Research of Energetic Materials Seminar*, Pardubice, Czech Republic, Apr. 25−27, 2007; Ottis, J. , Krupka, M., Eds.; University of Pardubice, Pardubice, Czech Republic, 2007; Vol. *2*, pp 532−540.
(36) Hammerl, A.; Hiskey, M. A.; Holl, G.; Klapötke, T. M.; Polborn, K.; Stierstorfer, J.; Weigand, J. J. *Chem. Mater.* **2005**, *17*, 3784–3793.
(37) Darwich, C.; Klapötke, T. M.; Welch, J. M.; Suceska, M. *Propellants, Explos., Pyrotech.* **2007**, *32*, 235–243.
(38) Klapötke, T. M.; Karaghiosoff, K.; Mayer, P.; Penger, A.; Welch, J. M. *Propellants, Explos., Pyrotech.* **2006**, *31*, 188–195.
(39) Grigoriev, M. S.; Moisy, P.; Den Auwer, C.; Charushnikova, I. A. *Acta Crystallogr.* **2005**, *E61*, i216–i217.
(40) Katrusiak, A.; Szafranski, M. *J. Mol. Struct.* **1996**, *378*, 205–223.
(41) Katrusiak, A.; Szafranski, M. *Acta Crystallogr.* **1994**, *C50*, 1161–1163.
(42) Steinhauser, G.; Crawford, M.-J.; Darwich, C.; Klapötke, T. M.; Miro Sabate, C.; Welch, J. M. *Acta Crystallogr.* **2007**, *E63*, o3100–o3101.
(43) Jin, X.; Shao, M.; Huang, H.; Wang, J.; Zhu, Y. *Huaxue Tongbao* **1982**, 336–337.
(44) Gaponik, P. N.; Ivashkevich, O. A.; Krasitskii, V. A.; Tuzik, A. A.; Lesnikovich, A. I. *Russ. J. Gen. Chem.* **2002**, *72*, 1457–1462.
(45) Klapötke, T. M.; Karaghiosoff, K.; Mayer, P.; Penger, A.; Welch, J. M. *Propellants, Explos., Pyrotech.* **2006**, *31*, 188.
(46) Morosin, B.; Dunn, R. G.; Assink, R.; Massis, T. M.; Fronabarger, J.; Duesler, E. N. *Acta Crystallogr.* **1997**, *C53*, 1609–1611.
(47) Charalambous, J.; Georgiou, G. C.; Henrick, K.; Bates, L. R.; Healey, M. *Acta Crystallogr.* **1987**, *C43*, 659–661.

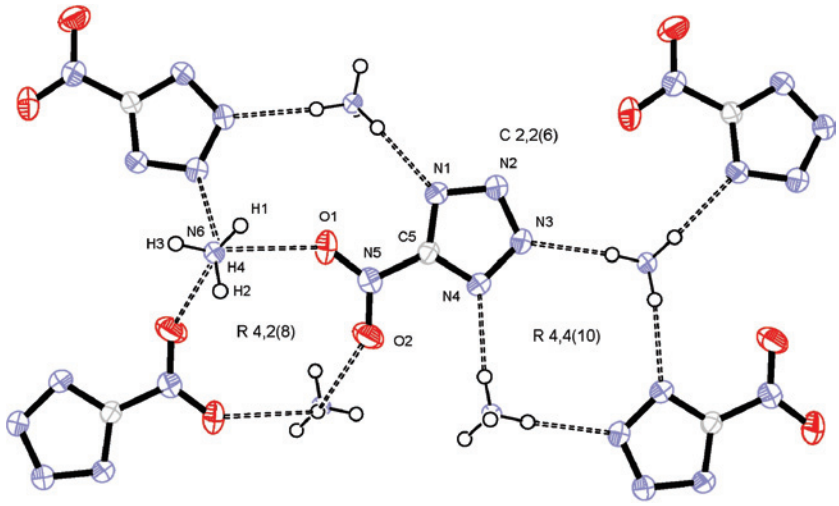

Figure 2. View normal to one layer of NT anions in **1**, including atom labels for the asymmetric unit, hydrogen bonds (dashed bonds), graph-set descriptors for prominent hydrogen bond patterns, and thermal ellipsoids showing 50% probability.

tetrazole portion of the NT anion in **1**−**6** is also very similar to other 5-substituted tetrazolate anions with electron-withdrawing substituents, including -CF_3[35,48,49] and -CN.[50,51] The tetrazole bond lengths in such tetrazolate anions are all ≈1.33 Å, and the angles are as expected for a slightly (symmetrically) distorted planar pentagon. As expected, the tetrazole ring bond lengths in 5-substituted tetrazolate anions with electron-withdrawing groups, such as NT, are slightly shorter than those in 5-substituted tetrazolate anions with electron-donating substituents, such as -NH_2.[52] The only geometric parameter in which significant variation is observed from one NT containing salt or metal complex to another, both in this study and in the literature, is in the "out-of-tetrazole-ring-plane" torsion of the nitro group. In Table 3 all four torsion angles describing the nitro group are listed for compounds **1**−**6**, and "out-of-tetrazole-ring-plane" torsions vary from 0° (**5**, NT moiety B) to 10° (**4**).

As suggested in the Introduction, intermolecular (or interionic) hydrogen bonding plays a pivotal role in determining the properties of energetic materials and is also the defining element of the structures of salts **1**−**6**. Not only is reasonably strong hydrogen bonding present in every structure in this study, but it also seems to contribute highly to the stability and density of these salts. Although compounds **2** and **6** are reasonably sensitive to friction and impact (Table 6), they are both much less sensitive than the heavy metal salts of NT (used as primary explosives) and considerably less sensitive than the alkali and alkaline earth metal salts and their hydrates.[53] Additionally, although the densities of

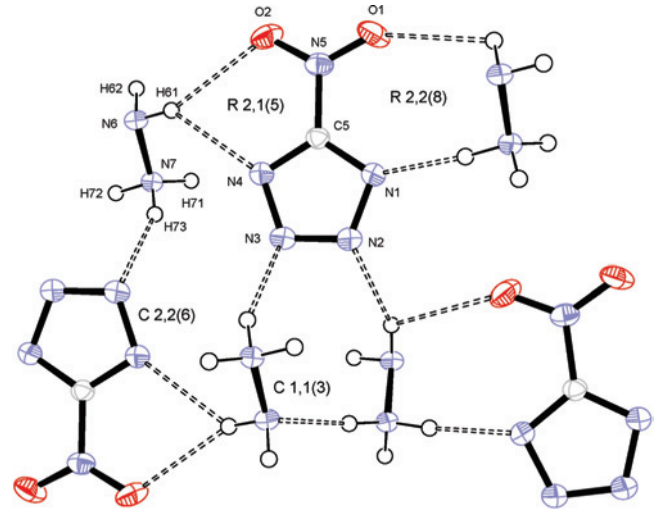

Figure 3. Hydrogen bonding in **2**, including atom labels for the asymmetric unit, graph-set descriptors, and thermal ellipsoids showing 50% probability.

1−**6** (∼1.6−1.7 g/cm^3) are not optimal (1.8−2.0 g/cm^3) for energetic materials, they are still reasonably high for salts composed of bulky organic cations and anions. In light of these points, a detailed description of the hydrogen-bonding and packing in **1**−**6**, using graph-set analysis as described by Bernstein et al.[54] and utilizing the computer program RPLUTO[55–57] is provided in the Supporting Information, Tables 2−7. In addition, the graph-set descriptors for common patterns are noted in Figures 2–8. Lastly, hydrogen bond geometric parameters and accompanying symmetry codes for compounds **1**−**6** are included in Supporting Information, Table 1.

Compound **1** crystallizes as described in Table 1 with planar layers of NT anions parallel to the crystallographic

(48) John, E. O.; Willett, R. D.; Scott, B.; Kirchmeier, R. L.; Shreeve, J. M. *Inorg. Chem.* **1989**, *28*, 893–897.
(49) Becker, T. M.; Krause-Bauer, J. A.; Homrighausen, C. L.; Orchin, M. *Polyhedron* **1999**, *18*, 2563–2571.
(50) Arp, H. P. H.; Decken, A.; Passmore, J.; Wood, D. J. *Inorg. Chem.* **2000**, *39*, 1840–1848.
(51) Graeber, E. J.; Morosin, B. *Acta Crystallogr.* **1983**, *C39*, 567–570.
(52) Ernst, V.; Klapötke, T. M.; Stierstorfer, J. *Z. Anorg. Allg. Chem.* **2007**, *633*, 879–887.
(53) Miró Sabaté, C. , Klapötke, T. M. , *Proceedings of The 10th New Trends in Research of Energetic Materials Seminar*, Pardubice, Czech Republic, Apr. 25−27, 2007; Ottis, J. , Krupka, M., Eds.; University of Pardubice: Pardubice, Czech Republic, 2007; Vol. *2*, pp 230−239.
(54) Bernstein, J. *Polymorphism in Molecular Crystals*, 1st ed.; Clarendon Press: Oxford, U.K., 2002.
(55) Motherwell, W. D. S.; Shields, G. P.; Allen, F. H. *Acta Crystallogr.* **2000**, *B56*, 466–473.
(56) *RPLUTO*, http://www.ccdc.cam.ac.uk/free_services/free_downloads/ (accessed Nov 24, 2007).
(57) Motherwell, W. D. S.; Shields, G. P.; Allen, F. H. *Acta Crystallogr.* **1999**, *B55*, 1044–1056.

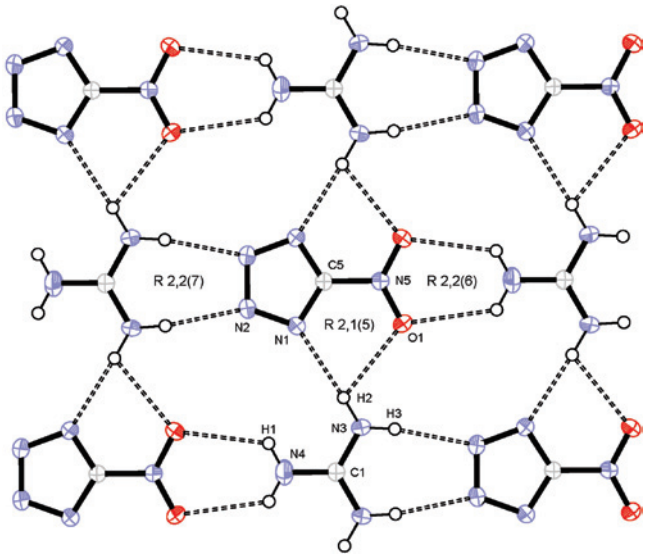

Figure 4. View normal to the *b*-*c* plane of a single layer of **3**, including atom labels for the asymmetric unit, hydrogen bonds (dashed bonds), graph-set descriptors for hydrogen bond patterns, and thermal ellipsoids showing 50% probability.

b-axis. Within the layers, the anions are joined to the tetrahedral ammonium cations (H1, H2, and H3 are also situated in the plane) by three strong hydrogen bonds as shown in Figure 2.

The crystal packing of **2** is defined by "stacks" of NT anions arranged such that planes defined by the tetrazole rings are parallel to one another, but the orientation of the nitro group alternates by ~180° between neighboring anions within the stack. The stacks formed are all parallel to the crystallographic *c*-axis, as well as to the hydrogen bonded (C 1,1(3) motif) chains of hydrazinium cations, which serve to connect (also by strong hydrogen bonding) the stacks of NT anions as shown in Figure 3.

The simplest packing in this study is found in the planar layer structure of **3**. The layers formed lie in the crystallographic *b*-*c* plane and with anion orientation alternating by 180° from layer to layer. Only four hydrogen bonds are present, because of symmetry, which connect the cations and anions within the layers. Between layers only weak van der Waals interactions predominate. The layered nature of the structure and the hydrogen bonding patterns in the structure of **3**, as shown in Figure 4, bear a strong but not wholly unexpected similarity to those found in guanidinium nitrate.[40,41]

Compound **4** exhibits complex packing, composed of neither layers nor stacks, in which each cation hydrogen bonds to six anions and vice versa. The cations and anions are either roughly parallel to or rotated ~50° out-of-plane from one another (see Figure 5 for packing details). Seven strong crystallographically independent hydrogen bonds (including the intramolecular hydrogen bond found in the aminoguanidinium cation) between the guanidinium and NT moieties and two additional weaker contacts are found between neighboring cations and O1 of the NT anion (Supporting Information, Table 1 and Figure 6).

5 crystallizes in the noncentrosymmetric space group $P2_1$ with 2 formula units per asymmetric unit (two cations and two anions). The two crystallographically independent cations are nearly parallel to one another and lie in the plane normal to the crystallographic *b*-axis. The planes of the tetrazole rings of the two anions are not parallel (twisted from each other by ~24 °) and lie approximately in the plane normal to the crystallographic *a*-axis. Therefore, the packing can be roughly described as being composed of perpendicular cations and anions. As in the structures of **1**−**4**, hydrogen bonding is the dominant feature of the packing in **5** (see Figure 7). However, because of the complexity and sheer number of crystallographically inequivalent hydrogen bonds (>17 depending on tolerances), a complete analysis of the hydrogen bonding network in **5** is not undertaken here.

As in **4** and **5**, the packing of **6** is composed of a complex three-dimensional hydrogen bonded network of cations and anions and is shown in Figure 8. Eleven crystallographically independent medium and strong hydrogen bonds are observed including three intraionic contacts similar to those found in **4** and **5**.

Energetic Properties. To assess the energetic properties of compounds **1**−**6**, the thermal stability (dehydration, melting, and decomposition points from DSC measurements) and sensitivity to friction, impact, electrostatic discharge, and thermal shock of each salt was experimentally determined (Tables 4 and 6). For each salt the constant volume energy of combustion was determined experimentally using oxygen bomb calorimetry and also predicted on the basis of calculated electronic energies (see computational methods section and Supporting Information, Table 9) and an estimation of lattice enthalpy[58,59] (Supporting Information, Table 10). Similar methods to the one used here for predicting thermochemical properties of energetic salts are described elsewhere.[17] However, for clarity details of the method used here are provided in the Supporting Information, Scheme 1. The measured and predicted thermochemical properties of **1**−**6** are summarized in Table 5. From the energies of formation (back-calculated from experimental combustion data), molecular formulas, and densities (from X-ray) the detonation performance parameters (pressure and velocity) for each compound were predicted using the EXPLO5 computer code.[60]

DSC measurements were made on samples of ~1 mg of each energetic compound in this study (**1**−**6**); they show melting points at or above 135 °C and decomposition points above 180 °C (Table 4). The trend in melting and decomposition points of **1**−**6** (**1** > **2** and **3** > **4** > **5** > **6**) is in keeping with known trends for simple nitrogen rich salts.[34,36] Because the salts in this study cannot (possibly excepting **6a**, T_m = 63 °C) be classified as ionic liquids, the melting points of the salts in this study are generally comparable to those for nonionic liquid heterocycle based salts of the NT anion and lower than those for metal salts of the NT

(58) Jenkins, H. D. B.; Tudela, D.; Glasser, L. *Inorg. Chem.* **2002**, *41*, 2364–2367.
(59) Jenkins, H. D. B.; Roobottom, H. K.; Passmore, J.; Glasser, L. *Inorg. Chem.* **1999**, *38*, 3609–3620.
(60) Suceska, M. *Propellants, Explos., Pyrotech.* **1991**, *16*, 197–202.

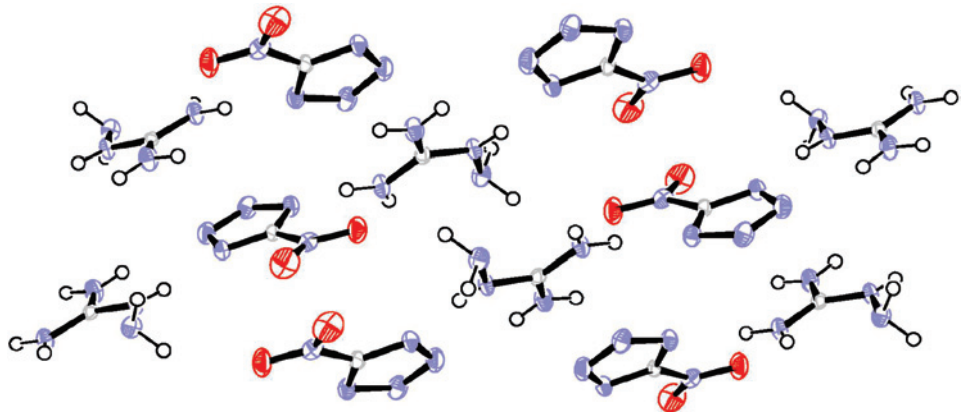

Figure 5. View of the packing in the unit cell of **4** along the crystallographic *b*-axis.

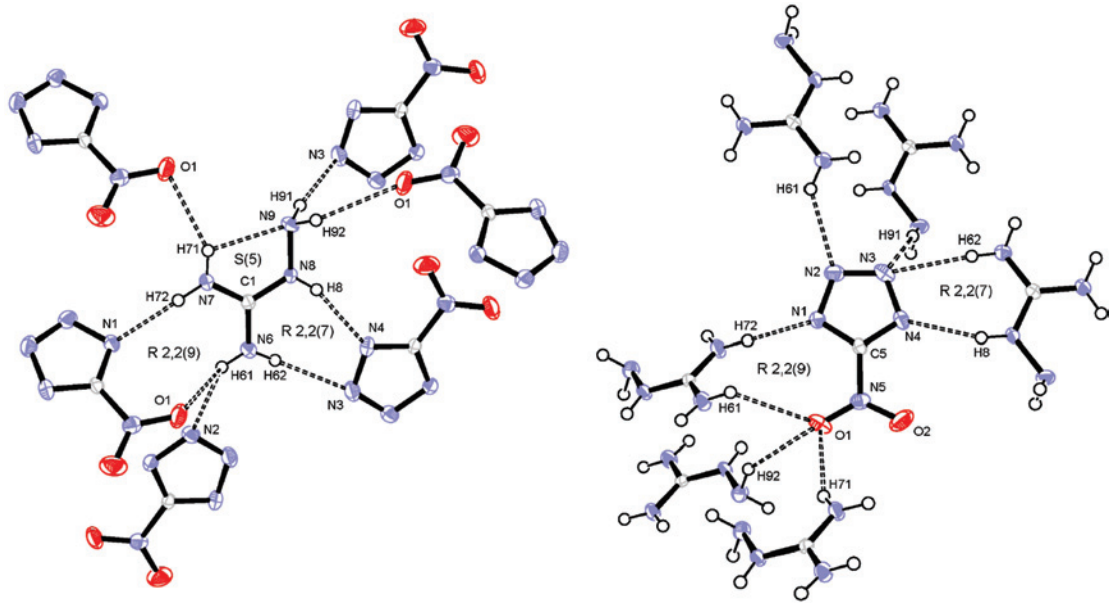

Figure 6. Hydrogen bonding around the cation (left) and anion (right) of **4**, including atom labels for relevant atoms, graph-set descriptors, and thermal ellipsoids showing 50% probability. Symmetry codes and geometric parameters for the hydrogen bonds shown can be found in Supporting Information, Table 1.

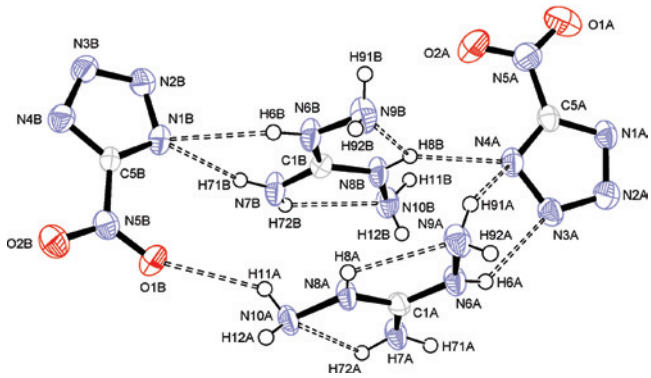

Figure 7. Hydrogen bonding in the asymmetric unit of **5**, including atom labels and thermal ellipsoids showing 50% probability.

anion.[6,8,9,11,18–20,43,53,61] The decomposition points of **1**−**6** are also similar to those of the heterocycle based salts (ionic liquids and solids) and are again lower than those for metal salts.[6,8,18–20,53] In comparison to commonly used explosives like TNT and RDX, **6** and **6a** have similar melting points to TNT (81 °C), and **1**−**5** have higher melting points than TNT and lower melting points than RDX (204 °C).[62] Compounds **1**−**6** decompose at lower temperatures than both RDX (230 °C) and TNT (300 °C). In addition to DSC analysis, all compounds were tested by placing a small sample (∼0.5−1 mg) of compound in the flame. In the case of **1**, **1a**, **2**, and **6**, the sample exploded. For **4**, **5**, and **6a** deflagration (rapid combustion, accompanied by a hissing sound) without explosion was observed, and **3** simply burns normally (both TNT and RDX detonate upon rapid heating). From these "flame test" observations it would seem that the compounds in this study composed of a higher percentage of nitrogen were more sensitive to thermal shock, as might be expected.

Data collected for friction, impact and electrostatic discharge sensitivity testing are summarized in Table 6. The compounds in this study are significantly less sensitive to friction and impact than known metal salts and complexes

(61) Talawar, M. B.; Chhabra, J. S.; Agrawal, A. P.; Asthana, S. N.; Rao, K. U. B.; Singh, H. *J. Hazard. Mater.* **2004**, *113*, 27–33.

(62) Koehler, J.; Mayer, R. *Explosivstoffe*, 9th ed.; Wiley-VCH: Weinheim, Germany, 1998.

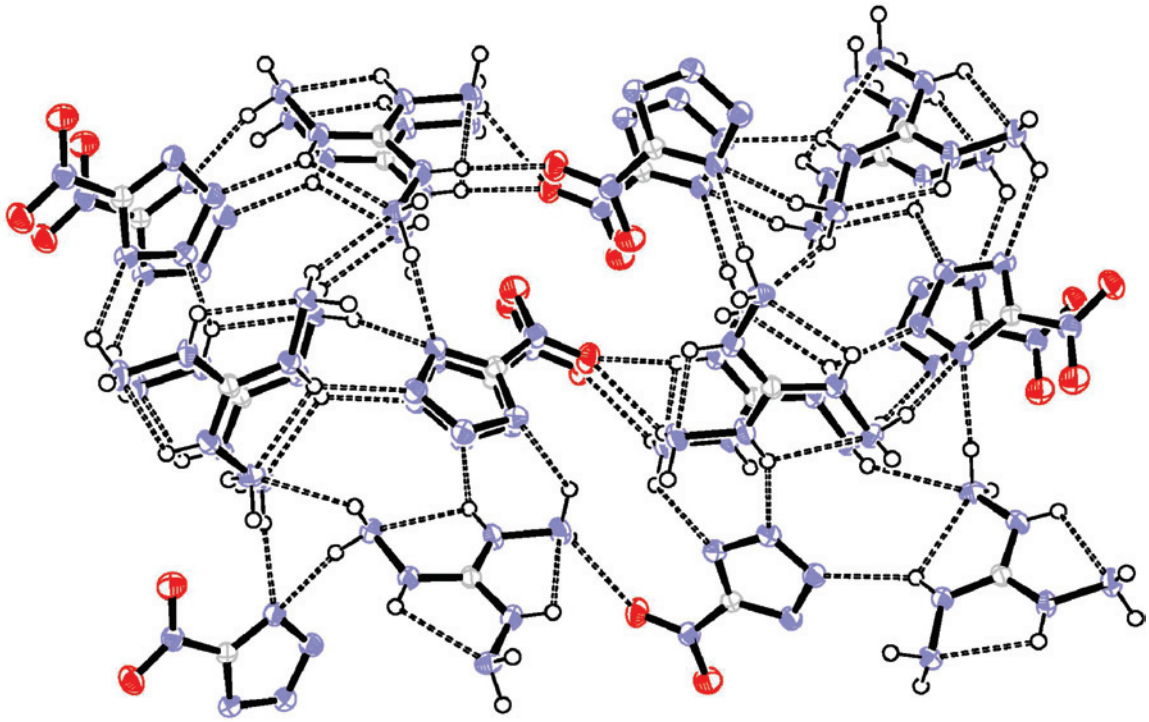

Figure 8. Packing and hydrogen bonding in **6** with thermal ellipsoids showing 50% probability.

Table 4. Physical Properties of **1**−**6**

	1	**1a**	**2**	**3**	**4**	**5**	**6**	**6a**
formula	$CH_4N_6O_2$	$CH_5N_6O_{2.5}$	$CH_5N_7O_2$	$C_2H_6N_8O_2$	$C_2H_7N_9O_2$	$C_2H_8N_{10}O_2$	$C_2H_9N_{11}O_2$	$C_2H_{11}N_{11}O_3$
T_m (°C)[a]	207	207	135	212	147	108	96	63
ΔH_{fus} (kJ/mol)[b]			−19.4		−33.4	−31.84	−26.6	−33.2
T_{deh} (°C)[c]		68						95
ΔH_{deh} (kJ/mol)[d]		10.7						1.43*
T_d (°C)[e]	210	217	188	217	211	216	191	191
N (%)[f]	63.6	59.6	66.7	64.4	66.7	68.7	70.3	65.0
Ω (%)[g]	−24.2	−24.2	−27.2	−45.9	−46.5	−47	−47.4	−47.4
ρ (g/cm^3)[h]	1.637	1.636	1.720	1.644	1.661	1.595	1.601	1.599

[a] Chemical melting point (DSC onset) from measurement with $\beta = 10$ °C/min. [b] Enthalpy of fusion from DSC measurement with $\beta = 10$ °C/min. [c] Temperature at which crystal water is lost (dehydration, DSC onset) from measurement with $\beta = 10$ °C/min. [d] Enthalpy of crystal water loss (dehydration) from DSC measurement with $\beta = 10$ °C/min. [e] Decomposition point (DSC onset) from measurement with $\beta = 10$ °C/min. [f] Percentage nitrogen. [g] Oxygen balance. [h] Density from X-ray measurements.

Table 5. Thermochemical Properties of **1**−**6**

	1	**1a**	**2**	**3**	**4**	**5**	**6**	**6a**
$\Delta_c U$(exp) (cal/g)[a]	−1860(30)	−1770(30)	−2110(150)	−2250(40)	−2470(30)	−2620(50)	−2690(50)	−2510(50)
$\Delta_c U$(pred) (cal/g)[b]	−2095.9	−1975.7	−2362.4	−2526.6	−2654.6	−2778.6	−2924.0	−2741.4
$\Delta_c H^o_m$(exp) (kJ/mol)[c]	−1030(20)	−1050(20)	−1290(90)	−1630(30)	−1940(20)	−2230(40)	−2460(40)	−2500(40)
$\Delta_c H^o_m$(pred) (kJ/mol)[d]	−1156.6	−1167.1	−1451.83	−1835.72	−2095.36	−2367.58	−2675.03	−2710.6
$\Delta_f H^o_m$(exp) (kJ/mol)[e]	60(20)	−70(20)	180(90)	−10(30)	160(20)	300(40)	390(40)	120(40)
$\Delta_f H^o_m$(pred) (kJ/mol)[f]	191.4	51.6	343.7	191.2	307.9	437.2	601.8	352.7
$\Delta_f U°$(exp) (kJ/kg)[g]	540(130)	−380(130)	1360(600)	30(160)	940(100)	1580(180)	1890(180)	650(180)

[a] Measured constant volume energy of combustion with standard deviations in brackets. [b] Predicted constant volume energy of combustion. [c] Standard molar enthalpy of combustion computed from experimental data with uncertainties in brackets. [d] Standard molar enthalpy of combustion computed from predicted data. [e] Standard molar enthalpy of formation computed from experimental data with uncertainties in brackets. [f] Standard molar enthalpy of formation computed from predicted data. [g] Standard energy of formation computed from experimental data with uncertainties in brackets.

of the NT anion.[11,14,44,53,63] Within the series of salts, **1**−**6**, a trend of increasing sensitivity to friction and impact with increasing nitrogen content is observed as was the case for the "flame test". Also, each compound was roughly tested for sensitivity to electrostatic discharge (ESD testing) by spraying sparks across a small (3−5 crystals) sample of material using a tesla coil (∼20 kV electrostatic discharge from an HF-Vacuum-Tester type VP 24). All compounds except **2** failed to explode under these conditions, indicating lower sensitivity to ESD than metal salts of the NT anion. Unfortunately, no data is recorded in the literature with regard to the sensitivity of heterocycle based NT salts, so no comparison can be made. Once again, comparison of the salts in this study to TNT and RDX is useful to assess their potential. Compounds **3**, **4**, and **6a** are less sensitive to both friction and impact than TNT and RDX as shown in Table

(63) Brown, M. E.; Swallowe, G. M. *Thermochim. Acta* **1981**, *49*, 333–349.

Table 6. Initial Safety Testing Results for and Predicted Energetic Performance of (EXPLO5 code) **1**−**6**, TNT, and RDX

	P_{det} (GPa)[a]	D (m/s)[b]	impact (J)[c]	friction (N)[c]	ESD (±)[d]	thermal shock
1	23.9	7950	**1** was not tested in bulk			
1a	22.5	7740	4	120	−	explodes
2	30.1	8750	2	16	+	explodes
3	20.1	7500	>30	>360	−	burns
4	24.7	8190	30	360	−	deflagrates
5	24.4	8230	4	360	−	deflagrates
6	26.0	8480	2	48	−	explodes
6a	20.7	7680	>30	>360	−	deflagrates
TNT	20.5	7100 (6900)	15	353	+	explodes
RDX	34.0	8900 (8700)	7.4	120	+	explodes

[a] Detonation pressure. [b] Detonation velocity, experimental values in parentheses.[62] [c] Impact and friction sensitivities determined by standard BAM methods.[65] [d] Rough sensitivity to 20 kV electrostatic discharge (ESD), + sensitive, − insensitive from an HF-Vacuum-Tester type VP 24.

6.[62] **5** is less sensitive to friction than TNT and RDX but more sensitive to impact than both TNT and RDX. The remaining materials (**1**, **1a**, **2**, and **6**) are as or more sensitive to impact and friction than RDX. Except for **2**, all compounds are less sensitive to electrostatic discharge than both TNT and RDX. Lastly, of the compounds in this study only **2** and **6** are not safe for transport under the U.N. Recommendations on the Transport of Dangerous Goods as described in ref 64.

In addition to safety considerations, performance of new energetic materials is of utmost interest. Using the molecular formula, density (from X-ray), and energy of formation ($\Delta_f U°$(exp)), the EXPLO5 computer code can be used to calculate the detonation velocity and pressure of CHNO explosives. Therefore, the energies of formation of **1**−**6** were back-calculated from constant volume energies of combustion by first converting to standard enthalpy of combustion and then on the basis of the general combustion equation for CHNO compounds, Equation **1**, Hess's Law as applied in eq **2**, incorporating the known standard heats formation for water and carbon dioxide[64] and a correction for change in gas volume during combustion (Equation **3**). Because of the reasonably large standard deviations for several sets of experimental combustion measurements, the thermochemical data ($\Delta_c U$, $\Delta_c H°_m$, $\Delta_f H°_m$, and $\Delta_f U°$) for each compound were predicted on the basis of known methods, utilizing calculated electronic energies and an approximation of lattice enthalpy,[17] in an attempt to validate the experimentally determined values.

$$C_aH_bN_cO_d(s) + \frac{4a-2d+b}{4}O_2(g) \rightarrow aCO_2(g) + \frac{b}{2}H_2O(l) + \frac{c}{2}N_2(g) \quad (1)$$

$$a\Delta_f H°_m(CO_2(g)) + \frac{b}{2}\Delta_f H°_m(H_2O(l)) - \Delta_c H°_m(C_aH_bN_cO_d(s)) = \Delta_f H°_m(C_aH_bN_cO_d(s)) \quad (2)$$

$$\Delta_f H°_m(C_aH_bN_cO_d(s)) - \Delta n_g RT = \Delta_f U°_m(C_aH_bN_cO_d(s)) \quad (3)$$

For compounds **1a** and **2**−**6**, calculation of $\Delta_f U°$(exp) may be calculated by the simple method described above and are tabulated in Table 5. However, for the hydrate **6a**, for which no combustion measurements were made, and anhydrous **1**, which was not studied in bulk, additional calculation (as outlined in the Supporting Information) is required to extract the experimental energies of formation of these materials.

As noted above, the standard deviations of the sets of five measurements used to experimentally determine the heat of combustion of each compound can be quite large (up to ~5%). The substantial uncertainties stem from several sources. First, and perhaps most significantly, all compounds in this study contain a large percentage of nitrogen and relatively little carbon or hydrogen; therefore, upon combustion relatively little energy is released, and very sensitive equipment would be required to detect such minute energy changes. To compensate for this, larger sample sizes would seem logical, but for safety reasons, as well as practical ones, the use of larger samples is not an effective solution. When larger samples or "concentrated" mixtures of compound and diluting agent (benzoic acid) are used for oxygen bomb calorimetric measurements, the samples tend not to combust cleanly but rather to explode. The explosion results in incomplete combustion and thus to less reliable measurements.

Therefore, as discussed above, the heats of combustion of all compounds were predicted by well established methods and are tabulated with the experimental data in Table 5. However, values for the hydrates **1a** and **6a** must be calculated taking into account the effect of crystal water on the lattice enthalpy. Once again, the procedure accounting for crystal water is detailed in the Supporting Information.

Also briefly of note, in their assessment of the above applied method for the prediction of the thermochemical properties of energetic salts, Gao et al.[17] predicted the heat of formation of **1**. Interestingly, the predicted and literature heats of formation found for **1** deviated by nearly 160 kJ/mol, yielding the poorest agreement between measured and predicted values for any compound found in the study of Gao et al. The predicted heat of combustion for **1** found in our study can be used to back-calculate a heat of formation for **1** of 163.6 kJ/mol, which agrees nicely with that predicted by Gao et al. (178.2 kJ/mol). The differences found are due to a difference in density values used for the lattice enthalpy prediction. The literature[22] value of 1.57 g/cm^3 was used by Gao et al., whereas we determined the density of **1** to be 1.637 g/cm^3 by X-ray analysis. However, the enthalpy of formation that can be calculated from our experimentally

(64) http://webbook.nist.gov.

(65) *UN Recommendations on the Transport of Dangerous Goods, Manual of Tests and Criteria.*, 4th ed.; United Nations: New York, 2003.

obtained heat of combustion for **1** of 70 ± 20 kJ/mol disagrees with our predicted value by ~110 kJ/mol, well within the range of deviation from predicted values found by Gao et al. This discrepancy seems to be explained by the fact that if the enthalpy of combustion for **1a** obtained in our study is treated as that of **1** and subsequently used to compute the heat of formation of **1**, a value of 10 ± 20 kJ/mol is calculated, which agrees nicely to the reported standard molar enthalpy of formation of **1**.[22] We feel that these observations along with the low reported density for **1** indicate the previously discussed misidentification of **1a** as **1**. Lastly, comparison of the values for the standard molar enthalpy of formation predicted and measured for **1** in this study seems to further validate the reliability of the method of Gao et al. for the prediction of thermochemical properties of energetic salts.

The explosion parameters for each compound were predicted on the basis of the theoretically verified experimentally determined energies of formation for each energetic salt. The EXPLO5 code was used using the following values for the empirical constants in the Becker−Kistiakowsky−Wilson equation of state (BKWN-EOS): $\alpha = 0.5$, $\beta = 0.176$, $\kappa = 14.71$, and $\theta = 6620$. The results of the calculations are shown in Table 6 along with the results of EXPLO5 calculations for TNT, RDX. From the EXPLO5 predictions made using the BKWN-EOS parameters given above and the known data for TNT and RDX, it would seem that detonation velocity and most likely pressure as well are slightly overestimated. Taking into account this systematic overestimation, the performance of all compounds assessed in this study is expected to fall between that of TNT (7100 m/s, 20.5 GPa) and that of RDX (8900 m/s, 34.0 GPa) (see Table 6).[62] In comparison to other 5-nitro-2*H*-tetrazole salts for which predicted performance data are reported, the salts in this study (excepting **3**) are predicted to perform as well as or outperform substituted triazolium salts (7500−7900 m/s, 20−25 GPa)[17,18,37] and methylated aminotetrazolium salts (6200 m/s, 15.5 GPa)[38] and with the exception of **2** under perform amino- and diaminotetrazolium salts (8840 m/s, ~31 GPa).[18] Lastly, it is important to point out that the data used to predict all literature performance values are based solely on theoretical heat of formation values predicted by the above-discussed methods. As shown in Gao et al. and here, these methods tend to systematically overestimate heat of formation values. Overestimation of heat of formation should lead to slightly exaggerated performance values. On the other hand, experimentally determined heats of formation, like those used in this study, tend to be underestimated for the above-mentioned reasons and therefore performance predictions based on experimental data should thus be slightly underestimated. Therefore, it seems that the compounds in this study should certainly perform as well as or slightly better than commonly used energetic materials.

Conclusion

A family of simple, nitrogen-rich energetic salts based on 5-nitro-2*H*-nitrotetrazole has been synthesized from readily available materials in moderate to excellent yields. Each salt was characterized fully, including X-ray structure determination. The vibrational frequencies of the NT anion were assigned on the basis of quantum chemical calculations to assist in a complete understanding of the vibrational spectra of all compounds studied. The hydrogen-bonded networks observed in the X-ray structures were assessed for strength and form (graph-set analysis). All salts in this study show good thermal stabilities (decomposition above 180 °C) but **1**, **1a**, and **3** lack good separation (~50 °C) of the melting and decomposition points. All compounds in this study have slightly negative oxygen balances. The densities of all of the salts are slightly lower than those desired for new high-performance energetic materials (1.8−2.0 g/cm^3) but are nonetheless in the range of currently used explosives (1.6−1.8 g/cm^3). All of the compounds, except **2** and **6**, are classified as less sensitive and **3** and **4** qualify as insensitive energetic materials. All compounds are predicted to perform at least as well as TNT and possibly as well as RDX. Several of the new salts in this study are promising candidates for further investigation, scale-up, and possible application as high-performance (**2** and **6**) or insensitive (**3** and **4**) energetic salts.

Acknowledgment. Financial support of this work by the Ludwig-Maximilian University of Munich (LMU), the Fonds der Chemischen Industrie (FCI), the European Research Office (ERO) of the U.S. Army Research Laboratory (ARL) and ARDEC (Armament Research, Development and Engineering Center) under contract nos. N 62558-05-C-0027, R&D 1284-CH-01, R&D 1285-CH-01, 9939-AN-01 & W911NF-07-1-0569 and the Bundeswehr Research Institute for Materials, Explosives, Fuels and Lubricants (WIWEB) under contract nos. E/E210/4D004/X5143 & E/E210/7D002/4F088 is gratefully acknowledged. The authors acknowledge collaborations Dr. M. Krupka (OZM Research, Czech Republic) in the development of new testing and evaluation methods for energetic materials and with Dr. M. Sucesca (Brodarski Institute, Croatia) in the development of new computational codes to predict the detonation parameters of high-nitrogen explosives. We are indebted to and thank Dr. Betsy M. Rice (ARL, Aberdeen, Proving Ground, MD) for many helpful and inspired discussions and support of our work. The authors also thank Dr. habil. Margaret-Jane Crawford for guidance and many insightful discussions.

Supporting Information Available: Crystallographic data in CIF format, tables of hydrogen bond geometries, graph-set matrices, computational results, thermodynamic details of standard molar enthalpy of combustion prediction and predicted thermochemical data (PDF). This material is available free of charge via the Internet at http://pubs.acs.org.

IC800353Y